Available online at www.ijpe-online.com

International Journal of Performability Engineering

vol. 14, no. 7, July 2018, pp. 1513-1520
DOI: 10.23940/ijpe.18.07.p15.15131520

A Novel Underwater Image Restoration Algorithm

Yongxin Wang[a,b] and Ming Diao[a,*]

[a]*College of Information and Communication Engineering, Harbin Engineering University, Harbin, 150001, China*
[b]*The Higher Educational Key Laboratory for Measuring and Control Technology and Instrumentations of Heilongjiang Province, Harbin University of Science and Technology, Harbin, 150080, China*

Abstract

This paper proposes a novel image restoration algorithm to eliminate light attenuation in underwater environments. The proposed algorithm employs the distance-dependent formation to model the degradation process where light travels in underwater. We use a homomorphic filter to get rid of the non-linear in the distance-dependent model. The restoration underwater image is then obtained by solving a Poisson equation that is derived based on the similar distance of neighbourhood pixels. The experiments show that the restoration image reveals improved contrast and clear details.

Keywords: underwater image restoration; homomorphic filter; distance-dependent model; Poisson equation

(Submitted on March 19, 2018; Revised on May 4, 2018; Accepted on June 7, 2018)

1. Introduction

High-class underwater images are the foremost element for exploitation of underwater resources. The primary constraint of underwater images is light attenuation when it travels in underwater [9]. Moreover, the ratio of light attenuation for each wavelength is different. For instance, the colour of the underwater image is biased towards blue and green rather than red because the attenuation of the red wavelength is most serious. The light attenuation leads to many difficult problems, such as failed colour constancy, low contrast, and blurring detail.

Recently, many contributions have been made to improve the quality of underwater images. Chiang [2] enhances underwater images by using a dehazing algorithm that is based on estimating the depth map. Galdran [4] proposes a red channel method, where colors associated with short wavelengths are recovered. The first step of Galdran's algorithm is to estimate the waterlight corresponding to the brightest pixel in dark channel. The second step is to estimate transmission from the dark channel, rather than estimate the depth map itself. Borker [1] proposes an underwater image enhancement method based on two sub-images fusion. The first sub image is derived using homomorphic filtering and contrast stretching. The second sub image is derived using adaptive histogram equalization and image smoothing. The final step of Borker's algorithm is to fuse the two sub-images by weights, which are computed using the principal component analysis. Zhao [12] extends this two sub image fusion method to the many sub image fusion method, where sub-images are obtained by some basic transformation function. Petit [7] firstly uses quaternions to process a color space contraction to inverse light attenuation. On this basis, Yang [11] adds the fuzzy morphological sieves to improve the non-uniform illumination condition.

In our work, we use the simplified hazy formation [8,10] to model the light attenuation process. This model uses Beer-Lambert law and path radiance to establish the correspondence relation between scene radiance and images captured by cameras. The residual energy ratio is employed to estimate the ratio of attenuation for each wavelength. The unknown distances of each pixel are overcome by exploring the difference in neighbourhood systems. Afterwards, a Poisson equation is derived due to the similar distance in the neighbourhood. Finally, the Poisson equation's solution which represents the unattenuated scene radiance is derived using the Jacobi iterative method.

* Corresponding author.
E-mail address: 51269528@qq.com

2. Underwater Imaging Model

The most popular underwater imaging model is the same as the model of a hazy image [10]. In Ran's work [8], this is called the distance-dependent model. The distance-dependent model consists of two components. The first model is the light attenuation part, which can be modelled by the Beer-Lambert law. The second model is called path radiance, which is also called backscattering. This second component is caused by ambient light. The overall underwater imaging model is given by Equation (1):

$$I_\lambda(x,y) = J_\lambda(x,y) \times t_\lambda(x,y) + \left(1 - t_\lambda(x,y)\right) \times A_\lambda \tag{1}$$

where (x, y) is the pixel position, λ represents a different wavelength channel, J is the scene radiance, I is the captured image, A_λ is the homogeneous background light, and t is the residual energy ratio. According to the Beer-Lambert law, residual energy ratio is a function of λ and the distance between the object and camera. The residual energy ratio t can be represented as follows:

$$t_\lambda(x,y) = 10^{-\beta(\lambda) \times d(x,y)} = N_\lambda^{d(x,y)} \tag{2}$$

where β is the medium's extinction coefficient, d is the distance, and N is the normalized residual energy ratio. By following the formation of the residual energy ratio in Equation (2), the distance-dependent model can be formulated as:

$$I_\lambda(x,y) = J_\lambda(x,y) \times N_\lambda^{d(x,y)} + \left(1 - N_\lambda^{d(x,y)}\right) \times A_\lambda \tag{3}$$

The normalized residual energy ratio N in Equation (3) is affected by water composition. In Duntley's work [3], oceanic water is divided into three categories. In Chiang's work [2], the following value is used to quantify the normalized residual energy ratio for most clear coastal waters:

$$N_\lambda = \begin{cases} 0.8 \sim 0.85, & \lambda = 650 \sim 750\ \mu m\ (r) \\ 0.93 \sim 0.97, & \lambda = 490 \sim 550\ \mu m\ (g) \\ 0.95 \sim 0.99, & \lambda = 400 \sim 490\ \mu m\ (b) \end{cases} \tag{4}$$

Note that in Equation (4), transmission of red wavelength decreases faster as distance increases. Therefore, the red channel is always described as the dark channel. According to Chiang's work [2], we can solve the background light A_λ by following Equation (5):

$$A_\lambda = \max_{(x,y) \in I} \min_{(i,j) \in \Omega(x,y)} I_\lambda(i,j) \tag{5}$$

3. The Proposed Algorithm

In this work, we propose a novel underwater enhancement algorithm. The block of the proposed algorithm is shown in Figure 1.

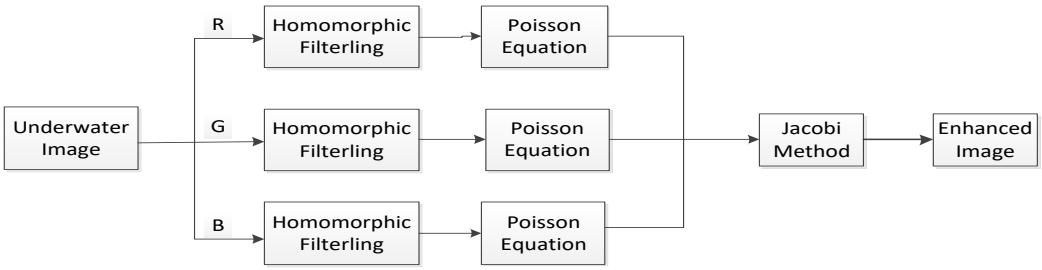

Figure 1. Block representation of the proposed algorithm

As shown in Figure 1, a homomorphic filter is performed for every wavelength channel. Then, we obtain three Poisson equations for each wavelength channel. Enhanced images are finally obtained using the Jacobi method. In the following sections, we illustrate the details of this block.

3.1. Underwater Imaging Model Linearity by Homomorphic Filtering

The underwater imaging model Equation (3) can be written as:

$$I_\lambda(x,y) = N_\lambda^{d(x,y)} \times \left(J_\lambda(x,y) - A_\lambda\right) + A_\lambda \tag{6}$$

Observing Equation (6), the distance d is part of the exponent. It is very difficult to obtain a numerical solution for this nonlinear relationship. We can use a logarithmic operation to remove the distance d from the exponent. Therefore, we put the logarithmic operation on both sides of Equation (6):

$$\log\left(I_\lambda(x,y) - A_\lambda\right) = \log\left(J_\lambda(x,y) - A_\lambda\right) + \log N_\lambda \times d(x,y) \tag{7}$$

This relationship provides a simpler expression than Equation (6) for the distance d.

3.2. Underwater Scene Radiance Estimation

As seen in Equation (7), the distance d and normalized residual energy ratio N are unknown. Although Equation (4) gives a range of normalized residual energy ratio N, we also need to estimate its exact value. Previous algorithms often prefer to estimate these two unknowns from degraded underwater I [5]. Unlike these algorithms, our algorithm recovers scene radiance without solving these unknowns. The adjacent pixels are always from the same object. The positions of adjacent pixels belonging to the same object are very close. Therefore, the distance between the observer and adjacent pixels is approximately equal.

However, the distances of adjacent pixels are slightly different due to the variant detail. However, the pixels' distances of the same local patch are homogenous. The most frequently used local patches are four neighbourhood and eight neighbourhood, whose weights are shown in Figure 2.

0	1	0
1	−4	1
0	1	0

(a)

−1	−1	−1
−1	8	−1
−1	−1	−1

(b)

Figure 2. (a) The weight of four neighbourhood (b) The weight of eight neighbourhood

Considering efficiency, we employ four neighbourhood, which is shown in Figure 1(a), as the local patch. Distance's homogeneity of the same local patch leads to Equation (8):

$$d(x,y) = 0.25 \times \left(d(x+1,y) + d(x-1,y) + d(x,y+1) + d(x,y-1)\right) \tag{8}$$

Let left-hand side is equal to $\tilde{J}_\lambda(x,y)$, and the first item of the right-hand side is equal to $\tilde{I}_\lambda(x,y)$. Then the following Equation (9) relation is obtained:

$$\tilde{J}_\lambda(x,y) = \tilde{I}_\lambda(x,y) + \ln(N_\lambda + c) \times d(x,y) \tag{9}$$

We also utilize the same relation for its neighbor. Then, the relation for every pixel is combined with the weight shown in Figure 1(a). Finally, we get the following Poisson:

$$\nabla^2 \tilde{J}_\lambda(x,y) = \nabla^2 \tilde{I}_\lambda(x,y) \tag{10}$$

where ∇^2 is Laplace operator. This is a linear system of equations about $\tilde{J}_\lambda$, which can be solved using the Jacobi iterative method. The intermediate results of the Jacobi iterative method are given by:

$$\tilde{J}_\lambda^{(n)}(x,y) = 0.25 \times \left(\tilde{J}_\lambda^{(n-1)}(x-1,y) + \tilde{J}_\lambda^{(n-1)}(x+1,y) + \tilde{J}_\lambda^{(n-1)}(x,y-1) + \tilde{J}_\lambda^{(n-1)}(x,y+1) - \nabla^2 I(x,y) \right) \quad (11)$$

where n represents the number of iterations. By repeating Equation (11), we can obtain the numerical solution of Equation (10). The solution is the estimation of the underwater scene radiance. The initial values of iteration are set in keeping with the degraded underwater image. Moreover, the mean squared error (MSE) is examined to check whether the iterative process is convergent.

4. Experimental Results

Our method is simulated by MATLAB 2016a on a desktop computer with an Intel i5-7500 CPU and Kingston 8G-DDR4 internal storage. The performance of the proposed algorithm is evaluated using objective assessment and subjective visual.

4.1. Test the Performance of Deblurring

In this section, we perform our algorithm for two test images with different blur. The enhanced image is obtained to test the performance of deblurring. We also show some intermediate results to verify the convergence of the proposed algorithm.

Figure 3 illustrates the performance of the proposed algorithm with moderate blur water. Figure 4 illustrates the performance of the proposed algorithm with immoderate blur water. As shown in Figure 3, the visual interference of degraded image is the blur that is caused by water medium. The proposed algorithm is capable of hazy removal. The vision of the enhanced image is less influenced by the blur. The result for immoderate blur water, shown in Figure 4, is poorer than the result shown in Figure 3. However, the image definition is improved significantly after performing the proposed algorithm.

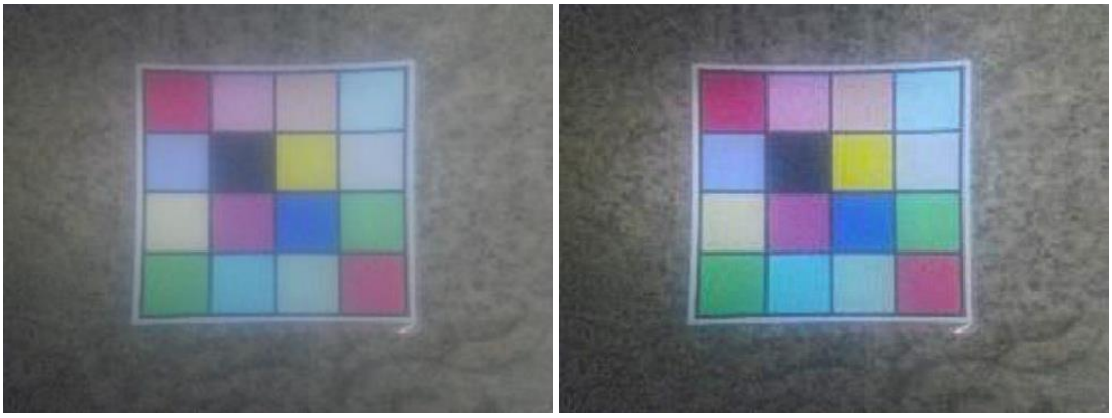

(a) (b)

Figure 3. (a) Original underwater image with moderate blur (b) Enhanced image using the proposed algorithm

(a) (b)

Figure 4. (a) Original underwater image with immoderate blur (b) Enhanced image using the proposed algorithm

Figure 5 shows the intermediate results for the immoderate blur image. As seen in Figure 5, the image becomes more vivid as the number of iteration increases. Using our algorithm, blur decreases and details gradually become more easily distinguished.

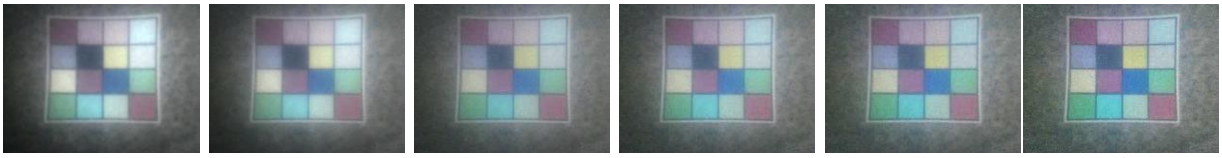

(a) (b) (c) (d) (e) (f)

Figure 5. The intermediate results for the immoderate blur image generated by the iterative process. The results from left to right correspond to the number of iterations: 1, 4, 7, 10, 13, 16

Figure 6 shows the value of entropy for immoderate blur images within 16 iterations. The iteration is a convergence process due to the shrinking value of MSE in pace with the iteration process shown in Figure 7. The value of entropy increases since the detail of the enhanced images is improved.

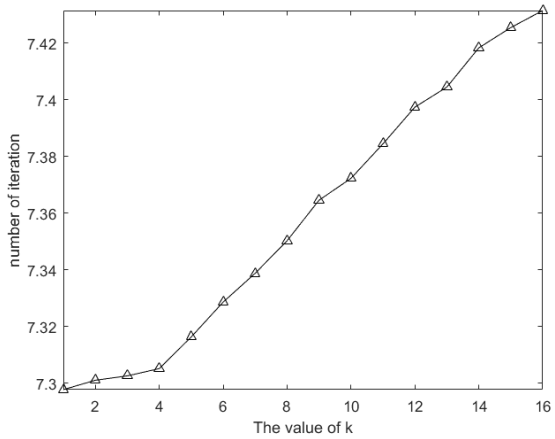

Figure 6. An illustration of the value of entropy with different numbers of iteration.

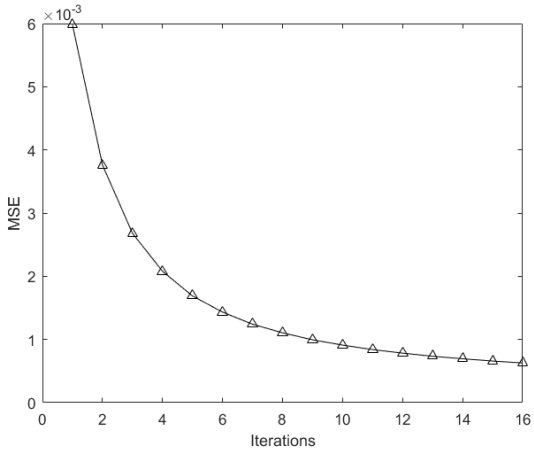

Figure 7. An illustration of the value of MSE with different numbers of iteration.

4.2. Visual Comparison and Assessment

In this section, we perform several image enhancement algorithms on two test underwater images. The subjective visual effect and assessment for the enhanced images are compared. The two test underwater images are shown in Figure 8. The visual comparison results are shown in Figure 9 and Figure 10.

(a) Shipwrecks (b) Waterweeds

Figure 8. Two test underwater images

(a) Chiang's result (b) Borker's result

(c) Galdran's result (d) Our result

Figure 9. A comparison of enhanced shipwrecks images

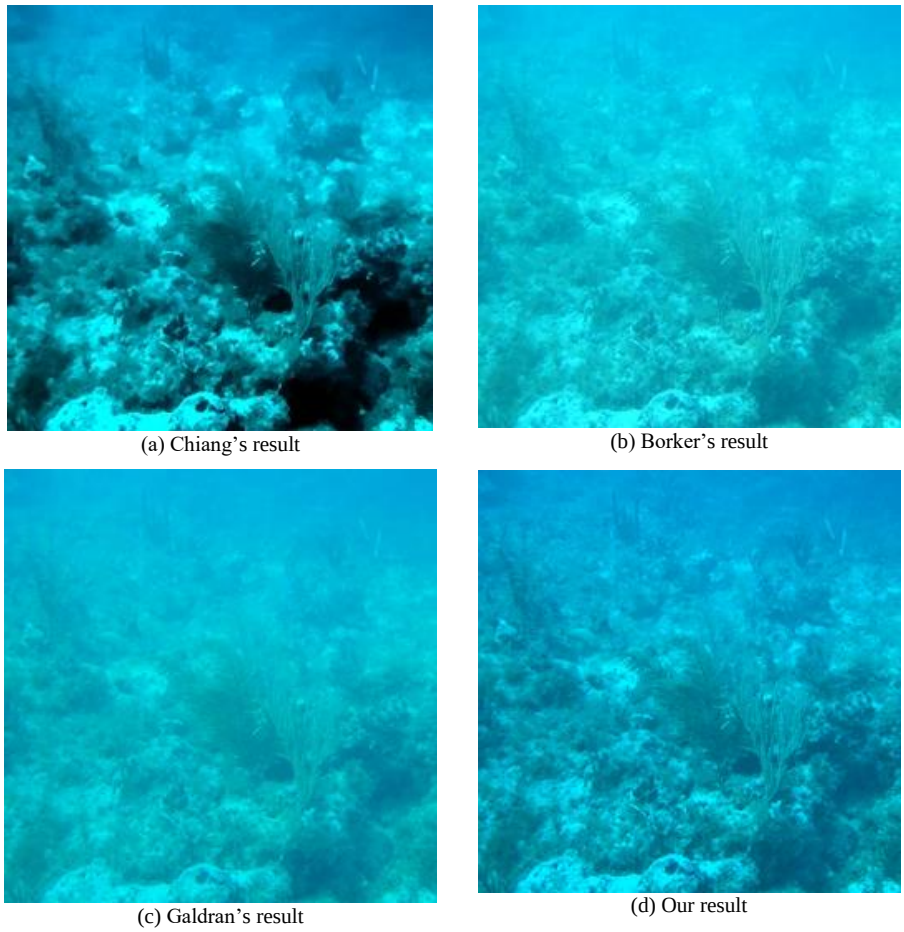

(a) Chiang's result (b) Borker's result

(c) Galdran's result (d) Our result

Figure 10. A comparison of enhanced waterweeds images

As shown in Figure 9 and Figure 10, the images obtained by the proposed algorithm obtain plausible results. The proposed algorithm exhibits a fine ability to improve contrast, enhance visibility, and remove blur. Moreover, the color of the enhanced images obtained using the proposed algorithm is corrected. Chiang's algorithm over-increases contrast. Consequently, the enhanced images obtained using Chiang's algorithm look unnatural. Borker's algorithm exhibits poor performance for deblurring. The detail of the enhanced images obtained using Borker's algorithm is still difficult to distinguish. Galdran's algorithm achieves a slightly clearer image. However, the definition of the enhanced images obtained using Galdran's algorithm are poorer than Figure 9 (d) and Figure 10 (d).

We choose entropy and the visible edge ratio metrics as the assessment to evaluate the image quality, followed by Li's work [6]. The entropy measures detail information and visual contrast. Low image quality has a lower value of entropy, and vice versa. The visible edge ratio takes into account the factor of edge. The value is equal to the ratio of the amount of edge invisible in the degraded image to the amount of edge visible in the enhanced image. The values of these assessments are shown in Table 1 and Table 2.

Table 1. The value of entropy and visible edge ratio of shipwrecks image

Compared algorithm	Entropy	Visible edge ratio
Chiang's algorithm	7.02	2.352
Borker's algorithm	6.58	0.441
Galdran's algorithm	6.91	1.315
Proposed algorithm	7.24	3.862

Table 2. The value of entropy and visible edge ratio of waterweeds image

Compared algorithm	Entropy	Visible edge ratio
Chiang's algorithm	6.87	1.784
Borker's algorithm	6.42	0.241
Galdran's algorithm	6.71	0.692
Proposed algorithm	7.09	3.245

Table 1 and Table 2 show the evaluation of every underwater image enhancement. The objective results are almost corresponding with the subjective visible, shown in Figure 9 and Figure 10. The proposed algorithm exhibits the best performance based on contrast enhancement, detail improvement, and searching hidden edges.

5. Conclusions

This paper focuses on recovering underwater scene radiance from degraded underwater images, which is disturbed by light attenuation and backscattering. Our work describes degraded underwater images using the distance-dependent model, which is widely used in blur removal and underwater image enhancement. We employ a homomorphic filter to transform the nonlinear model into a linearity equation. Based on the homogeneity of distance in the local patch, a Poisson equation is derived to recover the scene radiance, rather than separately estimate the distance and normalized residual energy ratio. The Jacobi iterative method is used to solve the Poisson equation. The solution is the enhanced underwater images. We test the proposed algorithm using subjective and objective views. The experiment results show that our algorithm performs more efficiently on enhanced details and contrast improvement.

References

1. S. Borker, and S. Bonde, "Contrast Enhancement and Visibility Restoration of Underwater Optical Images Using Fusion," *International Journal of Intelligent Engineering & Systems*, vol. 10, no. 4, pp. 217-225, April, 2017
2. J. Y. Chiang, and Y. C. Chen, "Underwater Image Enhancement by Wavelength Compensation and Dehazing," IEEE Transactions on Image Processing, vol. 21, no. 4, pp. 1756-1760, April, 2012
3. S. Q. Duntley, "Light in the Sea", *Journal of the Optical Society of Americ*a, vol. 53, no. 2, 214-233, February 1963
4. A. Galdran, D. Pardo, A. Picón, and A. Alvarez-Gila, "Automatic Red-Channel Underwater Image Restoration". *Journal of Visual Communication & Image Representation*, vol. 26, no C, pp. 132-145, January, 2015
5. K. He, J. Sun, and X. Tang, "Single Image Haze Removal Using Dark Channel Prior", *IEEE Transactions on Pattern Analysis & Machine Intelligence*, vol. 33, no. 12, pp. 2341-2353, December, 2011
6. C. Y. Li, J. C. Guo, B. Wang, R. M. Cong, and Y. Zhang, "Single Underwater Image Enhancement based on Color Cast Removal and Visibility Restoration", *Journal of Electronic Imaging*, vol. 25, no. 3, pp. 033012, March, 2016

7. F. Petit, A. S. Capellelaize, and P. Carre, "Underwater Image Enhancement by Attenuation Inversion with Quaternions", *Proceedings of the IEEE International Conference on Acoustics, Speech and Signal Processing* (ICASSP), pp. 1177-1180, Taipei, Taiwan, April, 2009
8. K. Ran, Y. Y. Schechner, and Y. Y. Zeevi, "Variational Distance-Dependent Image Restoration", *Proceedings of the IEEE Conference on Computer Vision and Pattern Recognition* (CVPR), pp. 1-8, Minneapolis, USA, June, 2007
9. N. B. Shamsuddin, B. W. Ahmad, B. B. Baharudin, B. M. Rajuddin, and F. B, Mohd, "Image Enhancement of Underwater Habitat Using Color Correction based on Histogram," Lecture Notes in Computer Science, Berlin, 2011
10. S. Shwartz, E. Namer, and Y. Y. Schechner, "Blind Haze Separation", Computer Vision and Pattern Recognition, *Proceedings of the IEEE Computer Society Conference on Computer Vision and Pattern Recognition* (CVPR), pp. 1984-1991, New York, USA, June, 2006
11. M. Yang, and Z. Ji, "Underwater Color Image Enhancement based on Quaternion and Fuzzy Morphological Sieves", *Chinese Journal of Scientific Instrument*, vol. 33, no. 7, pp.1601-1605, July, 2012
12. L. F. Zhao, A. L. Wang, B. Wang, and X. M. Lv. "Image Enhancement Algorithm based on Sub Image Fusion", *Systems Engineering and Electronics*, vol. 39, no. 12, pp. 2840-2848, December, 2017

Yongxin Wang received B.S. and M.S. degrees in Communication Engineering from Harbin University of Science and Technology, Harbin, China, in 2005 and 2010, respectively. His research includes underwater visual target recognition and embedded system design. He is currently a researcher at Harbin University of Science and Technology. Meanwhile, he is a Ph.D. student at Harbin Engineering University.

Ming Diao received a B.S. degree in Electronic Engineering from Harbin Institute of Shipping Engineering, Harbin, China, in1982. He received an M.S. degree in Communication and Information System from Harbin Institute of Shipping Engineering in 1987. His research includes wideband signal detection, processing and recognition, and digital communication. He is currently a professor at Harbin Engineering University.